

*A Peer Reviewed Refereed Journal*

## LUMINESCENCE CHARACTERISTICS OF MONOCLINIC ( $Ba_2MgSi_2O_7:Dy^{3+}$ ) PHOSPHOR

SANJAY KUMAR DUBEY<sup>A</sup>, SHASHANK SHARMA<sup>\*A</sup>, SANJAY PANDEY<sup>B</sup>, A. K. DIWAKAR<sup>A</sup>

<sup>a</sup> Dept. of Physics, Kalinga University, Naya Raipur, Chhattisgarh, India

<sup>b</sup> Dept. of Physics, Bhilai Institute of Technology, Raipur, Chhattisgarh, India

\*Corresponding Author: [dr.shashankeinstein@rediffmail.com](mailto:dr.shashankeinstein@rediffmail.com)

### ABSTRACT

$Ba_2MgSi_2O_7:Dy^{3+}$  (BMSD) white light emitting phosphor was sintered by traditional solid-state reaction process. The phase formation of the prepared phosphors was also confirmed through XRD characterization. Functional group investigation via FTIR spectroscopy and Photoluminescence properties were also studied. The results of the XRD study obtained for  $Ba_2MgSi_2O_7:Dy^{3+}$  (BMSD) phosphor revealed its monoclinic crystal symmetry with a space group C2/c. observed that the XRD pattern matched well with JCPDS file No. 23-0842. The average crystallite size was calculated as 30.51nm and strain as 0.29. The prepared phosphor was excited from 386nm and their corresponding emission spectra were recorded at blue (482 nm), yellow (574 nm) and red (675 nm) three spectral lines because of the  $^4F_{9/2} \rightarrow ^6H_{15/2}$ ,  $^4F_{9/2} \rightarrow ^6H_{13/2}$ ,  $^4F_{9/2} \rightarrow ^6H_{11/2}$ , transitions of  $Dy^{3+}$  ions. In this paper, the XRD, FTIR and photoluminescence properties of this phosphor are also discussed in detail.

**KEY-WORDS:** Solid-state reaction method; X-ray diffraction (XRD); Photoluminescence (PL),  $Ba_2MgSi_2O_7:Dy^{3+}$  (BMSD).

## 1. INTRODUCTION

The phenomenon of photoluminescence (PL) clearly indicates that it is the emission of light from a material under optical stimulation [1]. At present scenario, the sole purpose of research in the lightening markets and industries is to uncover that white light generated through light-emitting diode (LED) with the phosphors material [2]. This alkaline earth likewise calcium [Ca], strontium [Sr] and barium [Ba], RE (rare-earth) doped silicates have been

continuously investigated as long lasting luminescence-phosphors, to an increasingly market for their remarkable applications in various fields such as decoration, traffic signs and textile printing. From previous literature reports, it has been found that the silicate phosphors produce better characteristics likewise longer and brighter luminescence emission, facile preparation and cheaper, etc compare than previously utilized sulphide materials [3-7]. As activators, the probable advantages of lanthanide ions have now well ordered in the area of luminescence [8]. Jayasimhadri et al. (2010) & Verma et al. (2020) also reported that to white light generation, dysprosium ( $Dy^{3+}$ ) ion is well utilized as a do-pant in several host matrixes because it generates emission in the blue and yellow region of the visible spectrum [9-10]. The europium [ $Eu^{2+}$ ] doped di barium magnesium di silicate with luminescence spectrum exhibits superior emission intensity. ( $\lambda_{max} = 505$  nm) wavelength are an ideal for the human eye making the materials very appropriate to usual applications [11-12].  $Ba_2MgSi_2O_7$  phosphor has can be an excellent host material in which the probability of the excitation energy to be trapped by the killer center is lower [13-14]. This work is aimed at an assessment of optical properties of (3 mol %) dysprosium doped  $Ba_2MgSi_2O_7$  phosphor. In order to understand the structural formation such as XRD, FTIR and optical properties like PL spectra was also investigated of this phosphor.

## 2. EXPERIMENTAL STUDIES

### 2.1 Sample Preparation

Traditional solid-state reaction route is one of the best techniques as compared to other synthesis techniques. In this technique, high heating temperature is required [15]. We applied in our experiment,  $Ba_2MgSi_2O_7:Dy^{3+}$  (BMSD) were synthesized via solid-state reaction. All raw reagents with (99.99 %) purities such as  $BaCO_3$ ,  $MgO$ ,  $SiO_2 \cdot H_2O$  of Hi-media (AR Grade) and rare-earth in oxide form  $Dy_2O_3$  of Sigma-Aldrich (AR Grade). Very little quantity of (boric acid)  $H_3BO_3$  was taken as a flux. The stoichiometric ratio of the specimens using with acetone ( $CH_3COCH_3$ ) were grinded thoroughly in an agate mortar-pestle for 2 hour. After grinded sample was transferred in an alumina crucible. Sample was kept in programmable muffle furnace and then sintered at  $1100^\circ C$  for approximately 3 hours. The heating as well as the cooling rate of the furnace were set at  $5^\circ C$  per minute. Final phosphor (white powder) was acquired after additional crushing up to 1 hour. The resulting sample was restored in airtight bottle for characterization studies. Figure 1 displays the pure BMSD phosphor.

The chemical reaction of this process is given as follows:

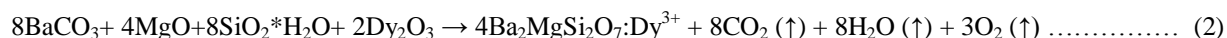
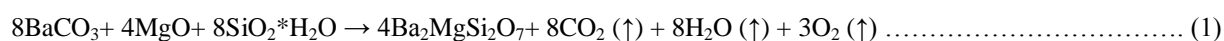




**Fig: 1 Pure  $\text{Ba}_2\text{MgSi}_2\text{O}_7$ :  $\text{Dy}^{3+}$  Phosphor**

## 2.2 Sample Characterization

X-ray diffraction (XRD) measurements were recorded with the help of Bruker D8 Advance X-ray diffractometer with  $\text{Cu-K}_\alpha$  radiation ( $\lambda=1.5406 \text{ \AA}$ , 40 kV, 40 mA) at room temperature. The vibrational properties of the sample have been performed using Bruker Alpha (transmission unit) Fourier Transform Infrared Spectroscopy. The photoluminescence (PL) data were collected with the help SHIMADZU, RF-5301 PC spectro-fluorophotometer provided. While performing the studies excitation and emission slit width were fixed at 3 nm. All experiments were performed in identical conditions and it was observed that the results were reproducible.

## 3. RESULTS AND DISCUSSION

### 3.1 X-ray diffraction (XRD)

XRD patterns of  $\text{Ba}_2\text{MgSi}_2\text{O}_7:\text{Dy}^{3+}$  phosphor synthesized by conventional solid state reaction method. It is recorded in the range of  $(10^\circ \sim 2\theta \sim 80^\circ)$ . Figure 2 displays the XRD pattern of pure BMSD phosphor. All the peaks showed well agreement matched with the help of JCPDS PDF file No. 23-0842 [16]. It is also examined that the influence of doping doesn't affect the phase structure of the phosphors. The cell volume  $V= 711 (\text{\AA})^3$  and the following lattice parameters:  $a = 8.4128 \text{ \AA}$ ,  $b = 10.7101 \text{ \AA}$ ,  $c = 8.4387 \text{ \AA}$ , and  $\beta = 110.71^\circ$  were also observed [17]. All parameters have shown in Table no. 1.

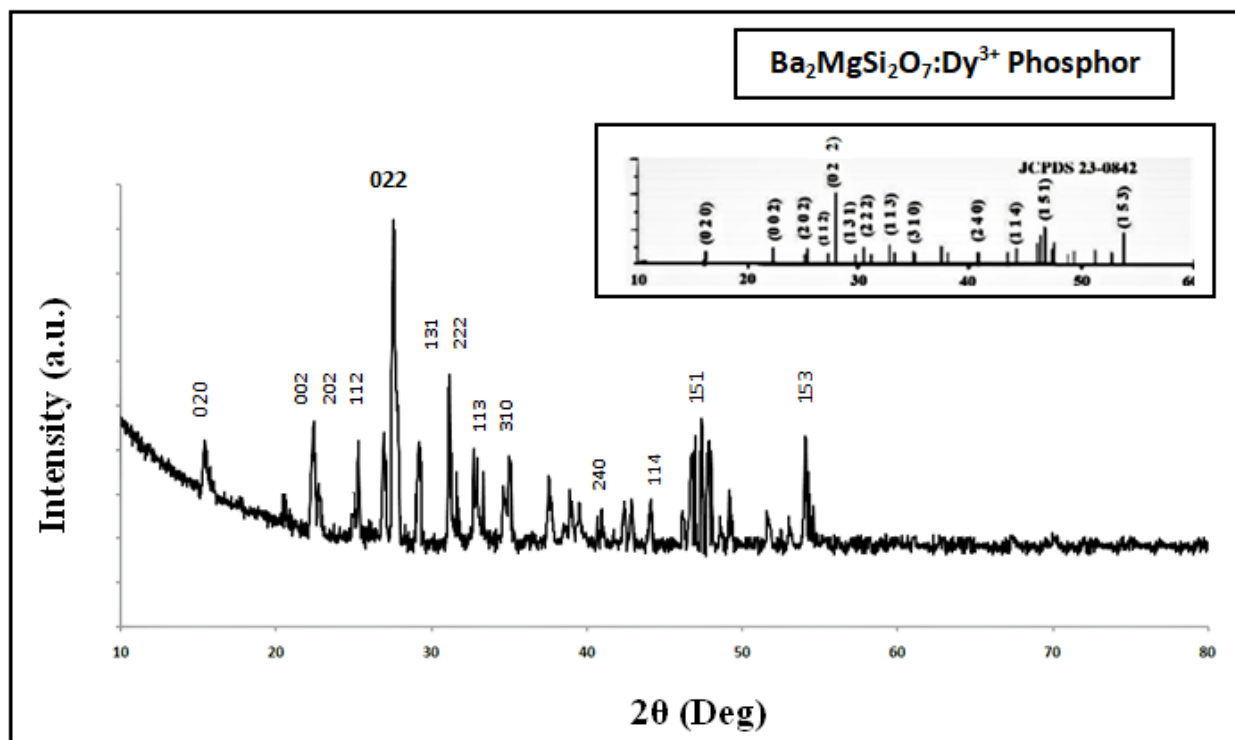


Fig. 2 XRD pattern of  $Ba_2MgSi_2O_7:Dy^{3+}$  phosphor.

### 3.2 Debye–Scherrer formula

The calculation of average crystallite size (D), with the help of Debye–Scherrer formula, for prominent peak (022) of the BMSD phosphor showed in table: 1.

Debye–Scherrer formula is represented as follows:

$$D = K\lambda / \beta \cos\theta \tag{3}$$

Where K = 0.94 (Scherrer constant),  $\lambda$  is wavelength of occurrence X-ray ( $\lambda = 1.5406 \text{ \AA}$ ),  $\beta$  is the FWHM (Full width half maximum) of the peaks and  $\theta$  (theta) is presented the corresponding Bragg's diffraction angle.

### 3.3 Strain Determination by Uniform Deformation Model (UDM)

The strain induced broadening in the powder sample was calculated via the following mathematical relation:

$$\varepsilon = \beta / 4 \tan\theta \tag{4}$$

**Table: (1)** According to the highest peak (022), position of the peak of the XRD patterns and the calculation values of the parameters.

No.	Parameters	Ba <sub>2</sub> MgSi <sub>2</sub> O <sub>7</sub> :Dy <sup>3+</sup> Phosphor
1.	Crystal Structure	Monoclinic
2.	Space Group	C2/c
3.	Lattice Parameters	$\beta = 110.71^\circ$ a = 8.4128 Å, b = 10.7101 Å, c = 8.4387 Å,
4.	Crystallite Size D(nm)	30.51nm
5.	2 $\theta$ [Deg]	27.49
6.	Cell Volume	711 (Å) <sup>3</sup>
7.	Crystal Plane Spacing d (Å)	3.24268 (Å)
8.	Strain	0.29

### 3.4 Fourier Transform Infra-Red Spectroscopy

#### 3.4.1 KBr Pallet Preparation

The KBr (potassium bromide) and BMSD sample pallet is displayed in fig. 3. Before recording the FTIR spectra of a synthesized sample, it is very essential to mix the synthesized sample with KBr (IR Grade) powder and grind it. After applying with hydraulic pressure to form a thin pallet. It is important to be note that KBr powder and BMSD sample should be in very little quantities. In this way, FTIR spectra and reading are acquired very clearly.



### Fig: 3 KBr and BMSD Sample Pallet

#### 3.4.2 FTIR Spectra

The FTIR spectrum of this pure BMS sample has been showed in fig: 3(c). This was recorded in the range of (4000  $\text{cm}^{-1}$  to 400  $\text{cm}^{-1}$ ). The band, centered at 483.52  $\text{cm}^{-1}$ , 565.19  $\text{cm}^{-1}$ , 619.33  $\text{cm}^{-1}$ , 676.35  $\text{cm}^{-1}$ , 837.63  $\text{cm}^{-1}$ , 923.36  $\text{cm}^{-1}$  and 1025.28  $\text{cm}^{-1}$  can be allocated to the responsible of silicate [ $\text{SiO}_4$ ] functional group. In addition, considering the absorption bands, validated at 676.35  $\text{cm}^{-1}$  and 565.19  $\text{cm}^{-1}$ , respectively, because of the responsible of [ $\text{SiO}_4$ ] functional group [18]. Thus examined, the absorption bands of silicate [ $\text{SiO}_4$ ] functional groups were clearly evident in the (IR) infra-red spectrum. The sharp band centered at 837.63, 923.36  $\text{cm}^{-1}$  and 1028.23  $\text{cm}^{-1}$  was allocated because of the responsible of Si-O-Si asymmetric stretch. The bands allocated at 676.35  $\text{cm}^{-1}$  and 619.33  $\text{cm}^{-1}$  may be responsible due to the [Si-O] symmetric stretching and [Ba-O] bending vibrations. The bands bending revealed at 565.19  $\text{cm}^{-1}$  and 483.52  $\text{cm}^{-1}$ , because of the existence of [Si-O-Si] vibrational mode. The Peak centered at 837.63  $\text{cm}^{-1}$  may be responsible to [Mg-O] bending vibrations and due to the asymmetric stretching on its spectrum dominates, band allocated at 1658.38  $\text{cm}^{-1}$ . The bands centered at 1829.50  $\text{cm}^{-1}$ , 1893.86  $\text{cm}^{-1}$  and 1969.33  $\text{cm}^{-1}$  is responsible because of the carbonation reaction mechanism. This can be lead to distortion in the lattice resulting in 1428.49  $\text{cm}^{-1}$  and 1658.38  $\text{cm}^{-1}$  vibration modes represented to vibration in divalent barium ion [ $\text{Ba}^{2+}$ ] and divalent magnesium ion [ $\text{Mg}^{2+}$ ] respectively. At 3454.43  $\text{cm}^{-1}$ , peak centered due to [O-H] hydroxyl group stretching which reveals the inherence of moisture in this specimen [19-25].

We get information about the inter-atomic distance and ionic radii from the literature of Shannon (1976). On the basis we are suggesting that in the host  $\text{Ba}_2\text{MgSi}_2\text{O}_7$  crystal structure, dysprosium ( $\text{Dy}^{3+}$ ) requires to acquisition of barium cation ( $\text{Ba}^{2+}$ ) site preferably. This is mainly because the ionic radius of dysprosium ( $\text{Dy}^{3+}$ ) (0.97 Å) is very close to that of Barium cation ( $\text{Ba}^{2+}$ ) (1.42 Å). But we also see that the ionic radius of magnesium cation ( $\text{Mg}^{2+}$ ) (0.58 Å) and silicon cation ( $\text{Si}^{4+}$ ) (0.26 Å) is very small. So both these cations are far away from the reach of dysprosium [ $\text{Dy}^{3+}$ ] [19].

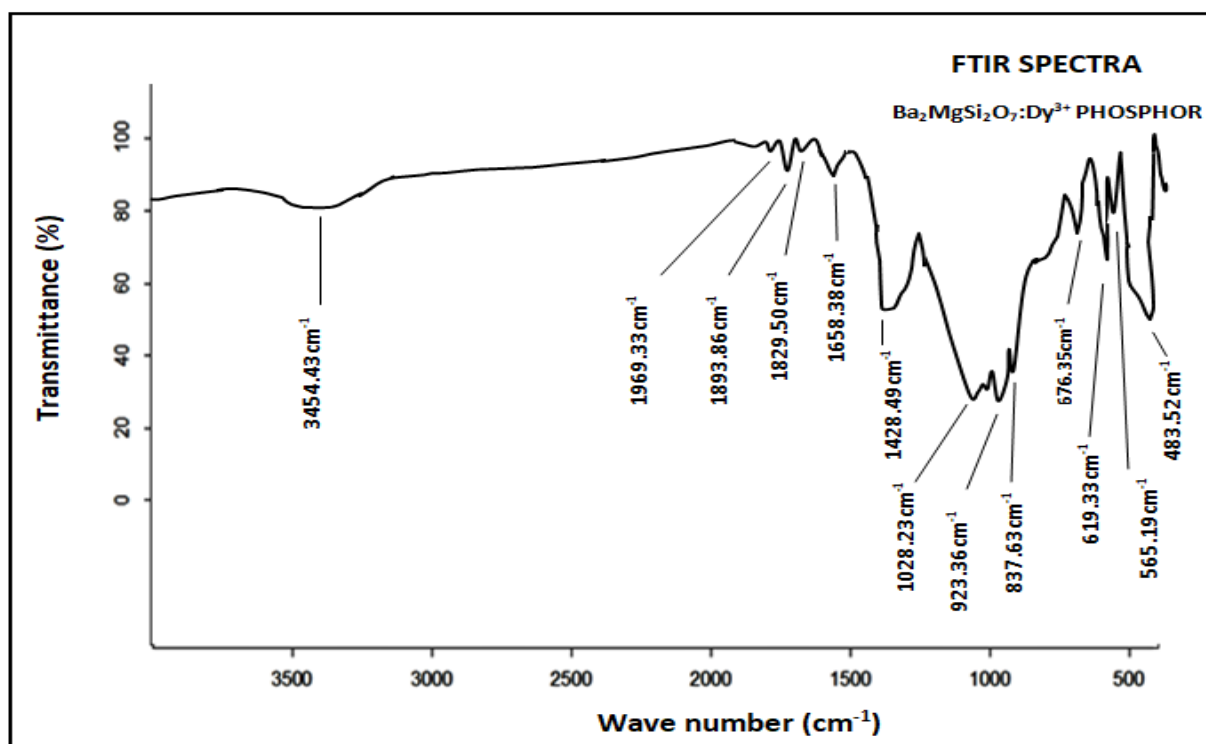


**Fig: 3(c) FTIR Spectra of Pure BMS Phosphor**

### 3.5 Photoluminescence Spectra

The excitation and emission spectra of Ba<sub>2</sub>MgSi<sub>2</sub>O<sub>7</sub>:Dy<sup>3+</sup> have presented in fig. 4(a) and 4(b) respectively. We see that a sequence of spectral lines is acquired in the range between (300 to 400nm) with the strongest peak at 386nm wavelength in the excitation spectra. Simultaneously, there are another two spectral lines peaking at 353nm and 338nm, wavelengths which are positioned to the transition from the lower energy state (ground state) to high energy state (excited states) in the 4f<sup>9</sup> configuration of dysprosium [Dy<sup>3+</sup>].



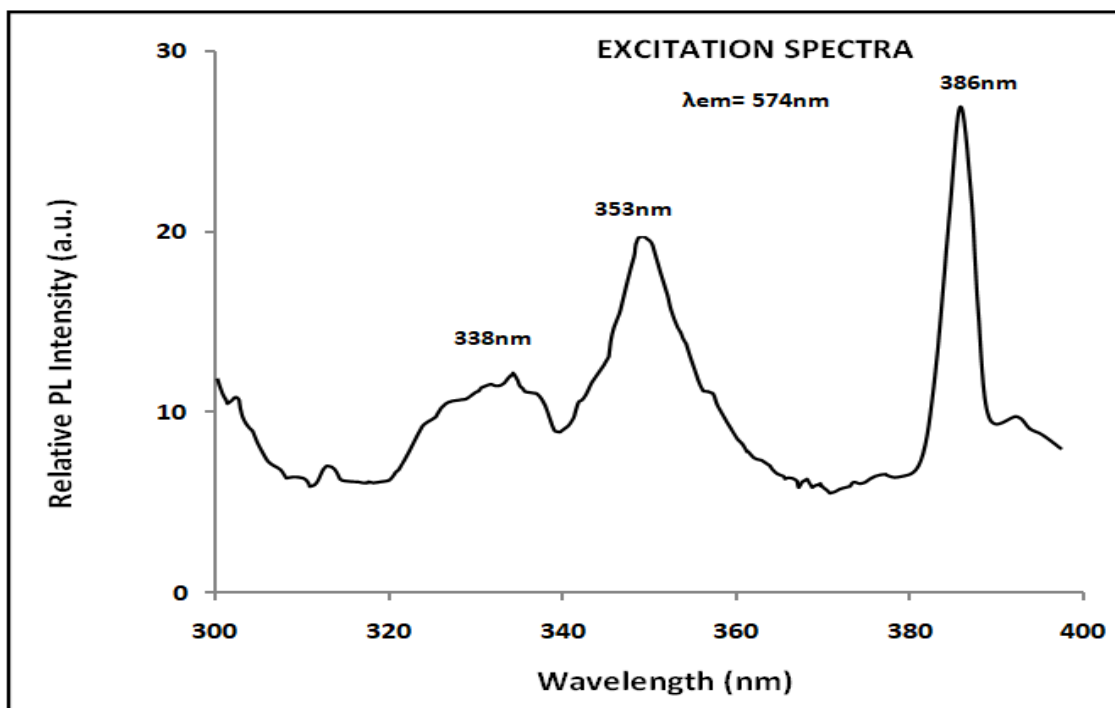


Fig: 4(a) Excitation Spectra- BMSD Phosphor.

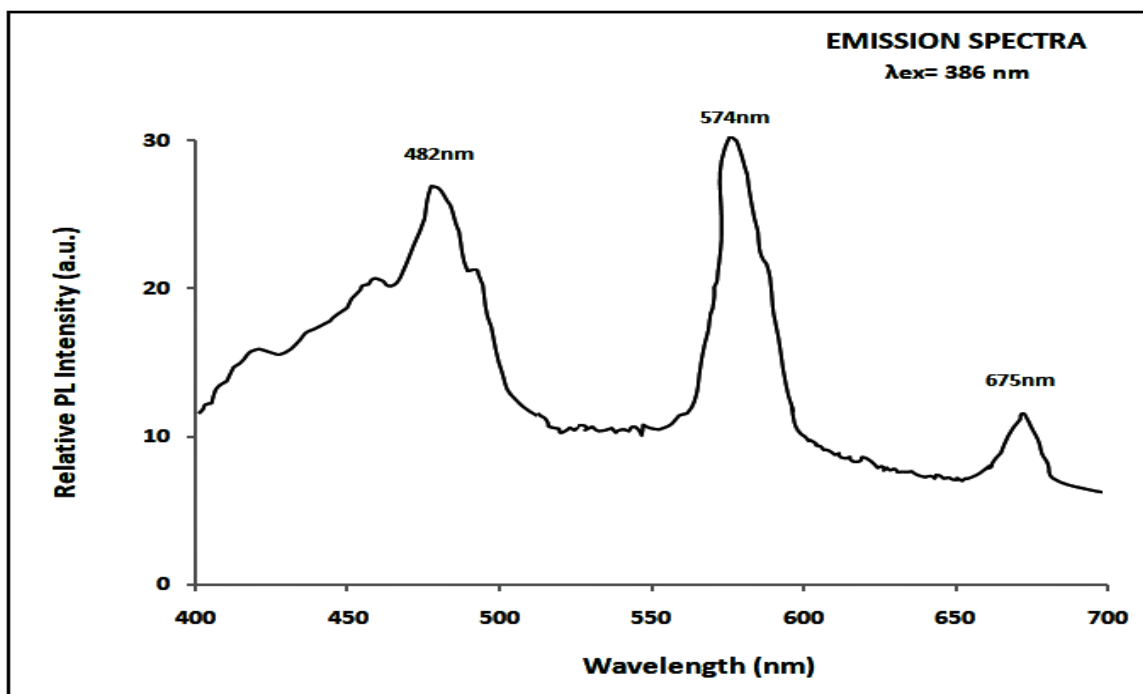


Fig: 4(b) Emission Spectra-BMSD Phosphor.

Fig. 5(b) is displaying the emission spectra of BMSD ( $\text{Ba}_2\text{MgSi}_2\text{O}_7: \text{Dy}^{3+}$ ) phosphor. At 359 nm wavelength, they were carried out under excitation spectrum in the range between (400 to 700nm). The emission spectra exhibited



intense spectral lines situated at 482nm ( ${}^4F_{9/2} \rightarrow {}^6H_{15/2}$ ), 574nm ( ${}^4F_{9/2} \rightarrow {}^6H_{13/2}$ ) and 675nm ( ${}^4F_{9/2} \rightarrow {}^6H_{11/2}$ ) because of the intra-configurational 4f–4f transitions of dysprosium [ $Dy^{3+}$ ] ion. The yellow ( ${}^4F_{9/2} \rightarrow {}^6H_{13/2}$ ) emission connected to the forced electric dipole transition type is permitted only at low symmetry. Synchronously, its intensity is strongly affected by the crystal-field surrounding. The blue band ( ${}^4F_{9/2} \rightarrow {}^6H_{15/2}$ ) is acquired because of the magnetic dipole transition 482nm wavelength and the red band ( ${}^4F_{9/2} \rightarrow {}^6H_{11/2}$ ) also acquired at 675nm wavelength in emission spectrum corresponds to the dysprosium [ $Dy^{3+}$ ] ion [26-28]. The optimum intensity is obtained with 3 mol % doping concentration of dysprosium [ $Dy^{3+}$ ] ion.

## CONCLUSION

In summary,  $Ba_2MgSi_2O_7:Dy^{3+}$  (3 mol %) phosphor was successfully synthesized via conventional high temperature solid state reaction synthesis. The XRD spectra of the phosphor were well matched through JCPDS file 23-0842. The synthesized phosphor was obtained in micro range with much better homogeneity. Actual formation and the functional group identification of the BMSD phosphor were collected via FTIR spectroscopy. The BMSD phosphor exhibited that the higher relative PL emission intensity peaks at (482 nm)  ${}^4F_{9/2} \rightarrow {}^6H_{15/2}$ , (574 nm)  ${}^4F_{9/2} \rightarrow {}^6H_{13/2}$  and (675nm)  ${}^4F_{9/2} \rightarrow {}^6H_{11/2}$  to electronic transition respectively. The optimal intensity acquired with a doping concentration of [3 mol %] dysprosium [ $Dy^{3+}$ ] ion. These results indicate that synthesized phosphor may be better promising candidate phosphor in the field of solid-state lighting and white light long afterglow applications.

## ACKNOWLEDGEMENTS

We gratefully acknowledge the kind support for the facility of XRD analysis Dept. of Metallurgical Engineering and FTIR analysis Dept. of physics, NIT Raipur (C.G.). Authors are also thankful to Dept of physics, Pt. Ravishankar Shukla University, Raipur (C.G.) for providing us the facility of Photoluminescence analysis. We are also heartily grateful to Dept. of physics, Dr. Radha Bai, Govt. Navin Girls College Mathpara Raipur (C.G.), providing the facility of muffle furnace and other essential research instruments.

## REFERENCE

1. Righini, G.C. and Ferrari, M., La Rivista del Nuovo Cimento, 2005, 28(12):1-53.
2. Laksh N., Vara U.V., J.Electrochem. Soc.,2005, 152(9):152-156.
3. MORAIS, VINICIUS R. de, DANIEL de R. LEME, and Chieko Yamagata. "Preparation of  $Dy^{3+}$ -doped calcium magnesium silicate phosphors by a new synthesis method and its luminescence characterization." (2018).

4. CHEN, Y.; CHENG, X.; LIU, M.; QI, Z.; SHI, C., J. Lumin., 2009, 129 ( 5):531-535.
5. FEI, Q.; CHANG, C.; MAO, D., J. Alloys. Compd., 2005, 390 (1-2):133-137.
6. HE, H, FU, R.; SONG, X.; LI, R; PAN, Z.; ZHAO, X.; DENG, Z.; CAO, Y., J. Electrochem. Soc., 2010, 157 ( 3):J69-J73.
7. CHANDRAKAR, P.; BISEN, D. P.; BAGHEL, R. N.; CHANDRA, B. P., J. Electron. Mater, 2015, 44(10):3450-3457.
8. CAI Jinjun, PAN Huanhuan and WANG Yi, RARE METALS, 2011, 30 (4):374.
9. B R Verma et al 2020 IOP Conf. Ser.: Mater. Sci. Eng. 798 012009.
10. Jayasimhadri M, Ratnam B V and Jang K, J. Am. Ceram. Soc, 2010, 93:494.
11. Shrivastava, R., Kaur, J., Dubey, V., Jaykumar, B. and Loreti, S., Spectroscopy Letters, 2015, 48(3):179-183.
12. Aitasalo, T.; Hreniak, D.; Holsa, J.; Laamanen, T.; Lastusaari, M.; Nittykoski, J.; Pelle, F.; Strek, W., J. Lumin., 2007, 122– 123:110–112.
13. J. Cai, H. Pan, W. Yi, Rare Metal., 2011, 30:374.
14. Sao, S.K., Brahme, N., Bisen, D.P., Tiwari, G. and Dhoble, S.J., Journal of Luminescence, 2016; 180:306-314.
15. S. Sharma, S.K. Dubey, International Journal of Scientific Research in Physics and Applied Sciences, 2021; 9(4):37-41.
16. JCPDS Pdf file number 23-0842, JCPDS International Center for Diffraction Data.
17. Aitasalo T., Hölsä J., Laamanen T., Lastusaari M., Lehto L., Niittykoski J., Pellé F: Z. Kristallogr. Suppl., 2006, 23:481-486.
18. Gou, Z.; Chang, J.; Zhai, W.; Journal of the European Ceramic Society, 2005; 25:1507–1514.
19. R.D. Shannon, Acta Cryst., 1976; A 32:751.
20. Qin. Fei, C. Chang, D. Mao, J. Alloy. Compd., 2005; 390 (1-2):134-137.
21. R.L. Frost, J.M. Bouzaid, B.J. Reddy, Polyhedron, 2007; 26:2405.
22. G.T. Chandrappa, S. Ghosh, K.C. Patil, J. Mater. Synth. Process., 1999; 7:273.
23. Makreski, G. Jovanovski, B. Kaitner, A. Gajovic, T. Biljan, Vib. Spectrosc., 2007; 44:162.
24. R. Caracas, X. Gonze, Phys. Rev. B, 2003; 68:184102.
25. M.A. Salim, R. Hussain, M.S. Abdullah, S. Abdullah, N.S. Alias, S.A. Ahmad Fuzi, M.N. Md Yusuf, K.M. Mahbor, Solid State Sci. Technol., 2009; 17(2):59–64.
26. Lin, L., Yin, M., Shi, C., & Zhang, W., Journal of Alloys and Compounds, 2008; 455(1-2):327-330.
27. Zhu, L., Zuo, C., Luo, Z., & Lu, A., Physica B: Condensed Matter, 2008; 405(21): 4401-4406.

28. Cheng, Y.; Cheng, Xu.; Liu, M.; Qi, Z.; Shi, C.; J. of luminescence, 2009; 129:531-535.